

# Total Angular Momentum Conservation During Tunnelling through Semiconductor Barriers

U. Gennser,<sup>(1)</sup> M. Scheinert,<sup>(2)</sup> L. Diehl,<sup>(2,3)</sup> S. Tsujino,<sup>(2)</sup> A. Borak,<sup>(2)</sup> C. V. Falub,<sup>(2)</sup> D. Grützmacher,<sup>(2)</sup> A. Weber,<sup>(2)</sup> D. K. Maude,<sup>(4)</sup> G. Scalari,<sup>(5)</sup> Y. Campidelli,<sup>(6)</sup> O. Kermarrec,<sup>(6)</sup> and D. Bensahel<sup>(6)</sup>

<sup>(1)</sup> CNRS-LPN, Route de Nozay,  
F-91960 Marcoussis, France

<sup>(2)</sup> Paul Scherrer Institut, CH-5232 Villigen, Switzerland

<sup>(3)</sup> Div. of Engineering and Applied Sciences,  
Harvard University, Cambridge, MA 02138, USA

<sup>(4)</sup> GHMFL, CNRS, F-38042 Grenoble France

<sup>(5)</sup> Université de Neuchâtel,  
CH-2000 Neuchâtel, Switzerland

<sup>(6)</sup> STMicroelectronics, F-38926 Crolles Cedex, France

(Dated: November 12, 2018)

We have investigated the electrical transport through strained  $p - Si/Si_{1-x}Ge_x$  double-barrier resonant tunnelling diodes. The confinement shift for diodes with different well width, the shift due to a central potential spike in a well, and magnetotunnelling spectroscopy demonstrate that the first two resonances are due to tunnelling through heavy hole levels, whereas there is no sign of tunnelling through the first light hole state. This demonstrates for the first time the conservation of the total angular momentum in valence band resonant tunnelling. It is also shown that conduction through light hole states is possible in many structures due to tunnelling of carriers from bulk emitter states.

PACS numbers: 72.25.Dc, 73.40.Gk

The challenge of introducing spin as an additional degree of freedom in semiconductor devices has lately attracted great attention.[1, 2] One approach to couple the spin to the carrier motion is through the spin-orbit interaction; one suggestion is to use it in conjunction with resonant tunnelling devices (RTDs) for injection and detection of spin currents.[3, 4] Whereas the spin-orbit coupling in the conduction band, mediated by the Dresselhaus mechanism [5, 6] or the Rashba mechanism,[7] is generally rather weak, the interaction is strong in the valence band. Since this band is made up from p-orbitals, the interaction term  $V_{so} \sim \mathbf{L} \cdot \mathbf{S}$  is non-zero, and there is a strong coupling between the orbital angular momentum  $\mathbf{L}$  and the spin  $\mathbf{S}$ , so that the total angular momentum  $J = L + S$  is a proper eigenvalue at the band edge. [8] In order to examine the feasibility of such devices for spintronics applications, one may therefore already consider spin (or  $J$ ) detection in p-RTDs. It is then rather disconcerting to find, that in all previous investigations, tunnelling has been observed from heavy hole states (HH; with  $(J, m_J) = (3/2, \pm 3/2)$  at  $k = 0$ ) to light hole states (LH;  $(3/2, \pm 1/2)$ ) or split-off states (SO,  $(1/2, \pm 1/2)$ ).[9, 10, 11, 12, 13] It has been proposed that this non-conservation of the total angular momentum  $(J, m_J)$  in resonant tunnelling is due to either the band mixing at finite in-plane momentum  $k_p$ , or because of interface roughness scattering. However, especially in strained quantum wells, the non-parabolicity and band mixing for the lowest states is quite small. This suggests that scattering plays a large role even in systems with interfaces known for their good quality. In our present study, we show the absence of resonances in the  $I - V$

characteristics from heavy holes tunnelling through the first light-hole state in a double barrier p-type quantum well. This demonstrates conclusively that there is  $\mathbf{J}$  conservation during resonant tunnelling. Furthermore, by investigating specially designed RTDs, we are able to show that the emitter structure away from the barrier interface may explain an apparent mixing of  $J$  in the tunnelling process.

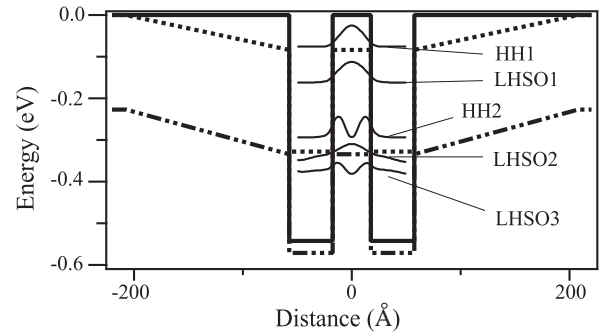


FIG. 1: Schematic Structure of the investigated RTD with a 35Å QW indicating the heavy hole valence band edge (filled line), light hole valence band edge (dotted line) and split-off band edge (dashed-dotted line).

The samples were grown by molecular beam epitaxy on fully relaxed  $Si_{0.5}Ge_{0.5}$  pseudosubstrates, of which the top 2  $\mu\text{m}$  is p-doped,  $p = 1 \times 10^{19} \text{cm}^{-3}$ . The active part of the initial structures consist of 40Å barriers surrounding a single  $Si_{0.2}Ge_{0.8}$  quantum well (QW) of width  $W$  ( $W = 25, 35, \text{ or } 45\text{Å}$  for three different sam-

ples). Symmetrically on either side of the active structure are 150Å thick SiGe emitter layers that are linearly graded, from 80% Ge closest to the barriers to 50% Ge away from the barriers. These emitter layers consists of an undoped spacer (100Å, closest to the barriers) and a doped part (50Å,  $p = 2 \times 10^{18} \text{cm}^{-3}$ ). A 2000Å,  $p = 2 \times 10^{18} \text{cm}^{-3}$  Si<sub>0.5</sub>Ge<sub>0.5</sub> top contact layer terminates the structure. The corresponding structure for the 35Å QW is schematically shown in Fig. 1. For clarity, the graded emitter region is also shown, and the lowest energy levels in the quantum well at  $k_p = 0$  are indicated. Due to the strain splitting, only HH states will be populated in the emitter closest to the barrier. Since the LH and SO bands are coupled even for zero in-plane momentum  $k_p$ , we have denoted these states as LHSO; however, the LHSO1 level is in fact predominately LH.

The diodes were processed into mesas with diameters varying between 10μm and 300μm. All measurements were performed at  $T \leq 4\text{K}$ , using separate voltage and current leads connected to both diode contacts, unless otherwise stated. However, we found that the resonance voltages changed by less than 10% between 4K and 77K.

In Fig. 2a the 77K current versus voltage characteristics of the three different RTDs are plotted. They show up to three resonances, with a maximum peak-to-valley current ratio of 5 : 1 at 4K. These characteristics are comparable to the best p-type RTDs in any material system, and indicate a good interface quality minimizing interface-roughness assisted tunnelling. In the following we will focus on the two lowest resonances.

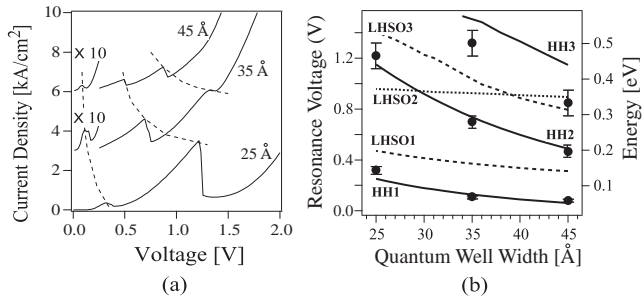


FIG. 2: (a)  $I - V$  characteristics at  $T = 77\text{K}$  of the RTDs with a 25Å, 35Å and 45Å quantum well. The curves for the 35Å and 45Å sample are shifted along the y-axis and magnified at the lowest voltages for clarity. The dashed lines are guides to the eye to follow the shift of the resonances. (b) Peak voltages vs. quantum well thickness (filled dots, left hand scale) and compared with quantum well levels calculated for an unbiased QW using a 6-band model (lines - HH states, dotted lines - LHSO states). The error bars indicate the variation between different diodes of the same structure. The left and right hand scales relate the energy and voltage to each other through the simple model described in the text.

The first evidence for assigning the resonances comes from the confinement shift clearly evident in the  $I - V$  characteristics. The shift, obtained from measurements of the smallest diodes, is unaffected by the contact layer

resistance from the substrate, as verified by the dependence of the current on the mesa size. In Fig. 2b the resonance voltages vs. well width are plotted. On the right hand scale, these are compared with the calculated energies. The scales can be directly compared by assuming a linear voltage drop across the double barriers, the quantum well and the undoped part of the structure. Including the Stark changes the energies much less than the measurement uncertainties. Because of the graded nature of the emitter, the zero bias emitter states lie  $\approx 30$  meV higher than the quantum well edge. This is included as an energy offset between the two scales. The so-called 'lever arm' - i.e. the ratio between the energy drop between the emitter and the centre of the quantum well and the applied voltage - is in good agreement with what can be expected from geometrical considerations, and the energies are consistent with those obtained from intersubband absorption measurements.[14] A good agreement between theory and experiment is found if the first two resonances correspond to tunnelling through the HH1 and HH2 states, respectively. Moreover, the difference between the first two resonances increases with decreasing well width. This effect is only obtained for states with different index, such as HH1 and HH2.

In view of the simplicity of the model - e.g. neither depletion width nor carrier accumulation in the structure is taken into account - this result alone can only be taken as an indication of the nature of the resonances. However, support for the model is found through magnetocurrent oscillations. For low, fixed  $V$  and with a magnetic field  $B$  applied parallel to the current, it is possible to observe weak oscillations periodic in  $1/B$  (period  $B_f$ ). They are due to Landau levels passing through the quasi-Fermi energy in the emitter accumulation layer, the two-dimensional charge density of which is  $p_e = 2eB_f/h$ . Unlike similar oscillations in GaAs/AlAs p-type RTDs [15], no decrease in  $B_f$  is found as  $V$  passes through the resonances, from which we conclude that the charge density in the quantum wells is negligible. Furthermore, the electric field  $F = ep_e/\epsilon\epsilon_0$  over the QW structure is in reasonable agreement with the simple lever arm model.

Further, conclusive evidence that the above assignment of the resonances is correct can be found in experiments where the resonances are shifted by a central potential spike. Even symmetry states (HH1, LHSO1), with a wave function maximum in the middle of the quantum well, are much more affected by a central, repulsive potential spike than odd symmetry states (HH2, LHSO2).[16] In our samples, the spike has been approximated by a thin Si layer; a 35Å QW with a 5Å spike in the middle was investigated and compared to the initial 35Å structure (Fig. 3a). The plotted wavefunctions in the figure give a clear picture of the described effect. An example of the  $I - V$  characteristics measured at 77K is displayed in Fig. 3b) and clearly demonstrate the predicted behaviour for the HH1 and HH2 states. We find shifts for the first and second resonances equal to  $(0.31 \pm 0.03)V$  and  $(0.06 \pm 0.08)V$ , respectively, where the uncertainty is due to the natural

scatter of the measured resonances for different diodes of the same structure. The values compares well with the calculated values (using the model described above, including Stark shifts) of  $0.21\text{V}$  and  $0.06\text{V}$  for the HH1 and HH2 resonance respectively.[17] In contrast, assuming a lever arm compatible with the second resonance due to LHSO1 tunnelling, the expected shift would be  $\geq 0.2\text{V}$ .

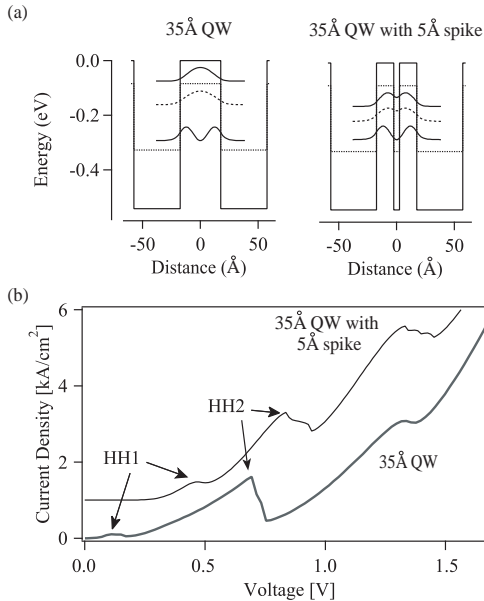


FIG. 3: (a) Schematic band diagrams of the  $35\text{\AA}$   $\text{Si}_{0.2}\text{Ge}_{0.8}$  quantum well without and with a central  $5\text{\AA}$  Si barrier, showing the HH and LH potential, and HH1, LHSO1 and HH2 wave functions. Only the HH2 state remains almost unaffected by the potential spike. (b)  $77\text{K}$   $I - V$  characteristics for samples with (shifted up for clarity) and without a central  $35\text{\AA}$  barrier. The resonances corresponding to tunnelling through the HH1 and HH2 states are indicated with arrows.

Having shown that it is possible to observe  $J$ -conservation in these tunnelling experiments, we now try to understand the difference between the present samples and those of previous studies, where tunnelling through LHSO states was observed. One important contrast is the higher strain used in the present study. For example, in previous studies of Si/SiGe RTDs on Si substrates, the Ge content was around  $20 - 25\%$ . [10, 13] One consequence is that the HH and LHSO states in the emitter were less decoupled in these samples, with a separation between the HH and LH potentials  $\leq 45\text{ meV}$ , whereas for the present samples it is  $\approx 85\text{ meV}$ . To study the role of the emitter, a structure with a  $25\text{\AA}$  QW and an emitter region with a grading from  $50\%$  to  $65\%$  was investigated (See Fig. 4(a)). Two resonances, at  $\approx 100\text{ mV}$  and  $\approx 470\text{ mV}$ , are observed in this 'emitter ramp' sample. The second resonance voltage is compatible with the estimated resonance voltage of the tunneling through HH2 but the first resonance is likely due to the tunneling through LHSO1: the tunneling through HH1 is prohib-

ited by design. Also the  $370\text{ mV}$  separation between the two resonances is more than a factor of 2 smaller than the separation between the HH 1 and the HH2 resonances of  $80\%$  emitter sample (Fig.2).

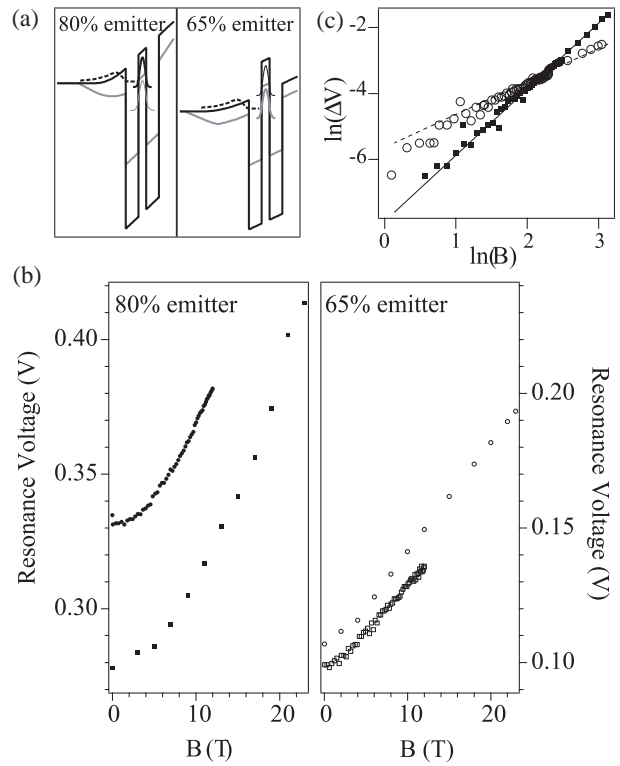


FIG. 4: (a) The schematic band diagram of the  $25\text{\AA}$  quantum well sample with an  $80\%$  emitter and a  $65\%$  emitter at biases close to their respective resonances. The HH potential (thick black line), the LH potential (thick grey), the quantum well HH1 (bold) and LHSO1 (grey) wavefunctions as well as the confined emitter state wave function (dashed) are shown. (b) The effect of a magnetic field parallel to the interface on the resonance voltages for the sample with a  $80\%$  and one with a  $65\%$  emitter. Two different diodes for each type of sample were measured up to  $12\text{T}$  and  $23\text{T}$  respectively, each with slightly different resonance voltage but with identical magnetic field behaviour. (c) Log of the resonance voltage difference  $\Delta V = V(B) - V(B = 0)$  vs. log of the magnetic field parallel to the interface, for the  $80\%$  (filled dots) and  $65\%$  emitter sample (open dots). Lines  $d(\ln(\Delta V))/d(\ln B) = 1$  and  $d(\ln(\Delta V))/d(\ln B) = 2$  are shown as guides for the eye.

To further compare these resonances, we use magnetotunnelling spectroscopy with  $B$  up to  $23\text{ T}$ . A magnetic field  $B_{\perp}$  applied perpendicular to the current  $I$  accelerates the carriers in the direction perpendicular to both  $B_{\perp}$  and  $I$ , so that they tunnel through the quantum well levels at a non-zero in-plane momentum, centered around  $\Delta k_p = q\Delta s B_{\perp}/\hbar$  where  $\Delta s$  is the tunnelling distance.[12] The in-plane dispersion relations can then be mapped out and compared with the calculated dispersion  $E(k_p)$ . [12, 13, 15, 18] All the HH1 resonances of the three regular structures show a parabolic behaviour.

The corresponding effective masses ( $0.04 m_0$ ,  $0.15 m_0$ , and  $0.13 m_0$  for the 25Å, 35Å and 45Å wells, respectively) are in reasonable agreement with the calculated dispersions ( $0.17 m_0$ ,  $0.155 m_0$ , and  $0.144 m_0$ ) though quantitative comparisons are difficult to make. [15]

In Fig. 4(b) we compare the  $B_{\perp}$  shift for the first resonance of the sample with a 25Å QW and an 80% emitter and of the emitter ramp sample. In contrast to the 80% emitter resonance, the first resonance of the emitter ramp sample shows a very distinct linear behaviour. A log plot clearly demonstrates these dependences (Fig. 4c). This indicates that it is the first resonance rather than the second that is not due to tunnelling through one of the HH states. Furthermore, a magnetic field  $B_{\perp}$  cannot lead to a linear energy shift of the valence band QW states or the emitter states next to the barrier. The Zeeman effect is given by  $E_Z = \kappa \mu_B \mathbf{J} \cdot \mathbf{B}$  (plus a small term proportional to  $B^2$ ) [19], which is only a small perturbation since the direction of  $J$  is frozen in the direction of the confinement and the strain. Since the well thickness is much smaller than the cyclotron orbit even for the highest fields, Landau level formation can also be excluded. Neither can the linear shift in Fig. 4 be explained by the acceleration in  $k$ -space, since the levels are quite parabolic, and never linear in  $k_p$ . In fact, we find that only an unstrained valence band bulk state can give rise to the observed linear shift. We propose that there are two reservoirs of holes in the emitter: states confined close to the Si barrier and states in the unstrained 'bulk' part of the emitter. The latter, tunnelling through the LHSO1 state, are responsible for the first resonance of the ramp emitter sample. In the bulk the  $\mathbf{J}$  vector is free to turn along the B-field axis, and with  $\mathbf{J}$  perpendicular to the growth axis, the quantum well state will 'see' a mixed HH-LHSO state coming from the emitter. Because of the lower Ge content in this emitter, the barrier for the holes from the bulk is smaller, making it possible for them either to tunnel directly into the quantum well states, or to form hybrid states with the emitter states in the HH emitter well. The Landau level separation in the  $\text{Si}_{0.5}\text{Ge}_{0.5}$  bulk is  $\approx 0.6$  meV/T, and the Zeeman energy a factor of 2-10 smaller.[20] This compares reasonably well with the measured slope of 4.1

mV/T  $\approx 1.4$  meV/T. It seems plausible that the apparent tunnelling from HH to LHSO states in other p-type RTDs may be due to the inevitable bulk part of the emitter, as well as band mixing in the well states. A similar linear behaviour has indeed been observed in a Si/Si<sub>0.75</sub>Ge<sub>0.25</sub> RTD with the strain fully in the SiGe layer. [18]

Concerning the third resonance of the 35Å and 45Å sample, the fit with the energy levels in Fig. 2 indicates that it corresponds to tunnelling through the second LH-like state (LHSO3 in the figure), and this also agrees with the observed shift in the sample with a central Si spike. This state is much less parabolic than the three lower states, and one would therefore expect a larger amount of band mixing. However, further experiments are necessary to confirm this.

We have demonstrated that the total angular momentum is conserved during resonant tunnelling in a system with strong spin-orbit coupling. This does not necessarily imply that the same holds true for the case of weakly coupled spin, but is certainly an encouraging sign. However, it may also have direct implications for the field of spintronics, since in order to inject spin in a semiconductor, a possible path is through the growth of magnetic semiconductors as electrodes. Much of the work has been focused on GaMnAs alloys, where the Mn not only provides the ferromagnetic properties, but also is a p-dopant.[21, 22] Finally, it should also be noted that these results may have an additional relevance for the development of a Si/SiGe based quantum cascade laser, in they exclude one of the possible non-radiative conduction paths for the HH carriers in these structures.[23]

## Acknowledgments

We would like to thank J. Faist for help with this work. It has been partly financially supported by the Swiss National Science Foundation, the EC Contract Si-GeNET, "Région Ile de France", "Conseil Général de l'Essonne" and the program Nano2008.

- 
- [1] G. Prinz, *Science* **282**, 1660 (1998).
  - [2] S. A. Wolf, *Science et al.*, **294**, 1488 (2001).
  - [3] K. C. Hall, *et al.*, *Appl. Phys. Lett.* **83**, 2973 (2003).
  - [4] M. M. Glasov, *et al.*, *cond-mat* 0406191 (2004).
  - [5] G. Dresselhaus, *Phys. Rev.* **100**, 580 (1955).
  - [6] F. Malcher, G. Lommer, and U. Rössler, *Superlatt. Microstr.* **2**, 267 (1986).
  - [7] Y. Bychkov and E. Rashba, *JETP Lett.* **39**, 78 (1984).
  - [8] J. M. Luttinger and W. Kohn, *Phys. Rev.* **97**, 869 (1965).
  - [9] E. E. Mendez, W. I. Wang, B. Ricco, and L. Esaki, *Appl. Phys. Lett.* **47**, 415 (1985).
  - [10] H. C. Liu, D. Landheer, M. Buchanan, and D. C. Houghton, *Appl. Phys. Lett.* **52**, 1809 (1988).
  - [11] R. M. Lewis, H. P. Wei, S. Y. Lin, and J. F. Klem, *Appl. Phys. Lett.* **77**, 2722 (2000).
  - [12] R.K. Hayden, *et al.*, *Phys. Rev. Lett.* **66**, 1749 (1991).
  - [13] U. Gennser, *et al.*, *Phys. Rev. Lett.* **67**, 3828 (1991).
  - [14] L. Diehl, *et al.*, *Appl. Phys. Lett.* **80**, 3274 (2002).
  - [15] R.K. Hayden, *et al.*, *Semicond. Sci. Technol.* **7**, B413 (1992).
  - [16] J.-Y. Marzin and J.-M. Gérard, *Phys. Rev. Lett.* **62**, 2172 (1989).
  - [17] The larger discrepancy for the HH1 is expected since it is more sensitive to the exact thickness of the Si spike.
  - [18] P. Gassot, *et al.*, *Physica E* **2**, 758 (1998).
  - [19] J. M. Luttinger, *Phys. Rev.* **102**, 1030 (1956).
  - [20] The value depends on the interpolation used between Si and Ge. See R. Winkler, M. Merkler, T. Darnhofer, and

- U. Rössler, Phys. Rev. **B 53**, 10858 (1996).
- [21] T. Dietl, *et al*, Science **287**, 1019 (2000).
- [22] R. Mattana, *et al*, Phys. Rev. Lett. **90**, 166601 (2003).
- [23] U. Gennser, *et al*, in 'Future Trends in Microelectronics',  
Ed. S. Lyuri, J. Xu, and A. Zaslavsky (Wiley-IEEE Press,  
2004).